VOLUME 116, NUMBER 2
JANUARY 26, 1994

JOURNAL
OF THE
AMERICAN
CHEMICAL
SOCIETY

Conformational Analysis of the δ Receptor-Selective, Cyclic Opioid Peptide, Tyr-*cyclo*[D-Cys-Phe-D-Pen]OH (JOM-13). Comparison of X-ray Crystallographic Structures, Molecular Mechanics Simulations, and ^{1}H NMR Data

Andrei L. Lomize,† Judith L. Flippen-Anderson,‡ Clifford George,‡ and Henry I. Mosberg*,†

Contribution from the College of Pharmacy, University of Michigan, Ann Arbor, Michigan 48109, and Laboratory for the Structure of Matter, Code 6030, Naval Research Laboratory, Washington, D.C. 20375

Received September 1, 1993®

Abstract: The conformational features of the δ-selective, cyclic opioid peptide Tyr-*cyclo*[D-Cys-Phe-D-Pen]OH (JOM-13) were investigated using a combination of experimental (X-ray crystallography, ^{1}H NMR spectroscopy) and theoretical (molecular mechanics computations) techniques. Energy calculations with the CHARMm force field show the existence of a single energetically preferred backbone conformation for the cyclic tripeptide portion of the molecule. Several distinct low-energy conformations were calculated, however, for the disulfide bridge linking the D-Cys and D-Pen residues, for the single Tyr residue outside the cycle, and for the Tyr and Phe side chains. The two calculated lowest-energy conformers of the D-Cys, D-Pen disulfide bridge (A and B) differ in values of D-Cys χ^1 and χ^3 (S–S) torsion angles (the –60°,90° and 180°,–90° combinations). This is consistent with the observation of two ^{1}H NMR signal sets in aqueous solution (in the ratio 68:32) with distinctly different vicinal coupling constants for protons H-C$^\alpha$C$^\beta$-H that correspond to a D-Cys χ^1 angle of about –60° for the first set and ~180° or +60° for the second. X-ray crystallographic analysis of crystals grown from aqueous solution also revealed two independent conformers which are in excellent agreement with the computational and NMR data for the rigid, cyclic part of the molecule including the disulfide bridge. However, ^{1}H NMR data and computational results indicate that the flexible elements of JOM-13 (the exocyclic Tyr residue and the Tyr and Phe side chains) have no fixed structure in water solution. In the crystalline environment they adopt conformations that are stabilized mainly by intermolecular interactions and which do not correspond exactly to any local energy minimum identified in the molecular mechanics calculations.

Introduction

Soon after the discovery, in 1975, of the endogenous opioid peptides Leu- and Met-enkephalin,[1] the first of many studies aimed at deducing the bioactive conformation(s) of these compounds was initiated. Over the years it has become clear that this goal is a most difficult one, and, indeed, the efforts of many laboratories remain focused upon it. Several factors contribute to this difficulty, some of which stem from the unavailability of sufficient quantities of purified opioid receptor of either the μ- or the δ-type (those receptors to which the enkephalins show significant binding affinity) capable of high-affinity ligand binding. This then renders impossible the gathering of direct evidence for the bioactive conformation. Instead, only

* To whom correspondence should be addressed.
† University of Michigan.
‡ Naval Research Laboratory.
® Abstract published in *Advance ACS Abstracts*, January 1, 1994.
(1) Lord, J. A. H.; Waterfield, A. A.; Hughes, J.; Kosterlitz, H. W. *Nature* **1977**, *267*, 495–499.

0002-7863/94/1516-0429$04.50/0

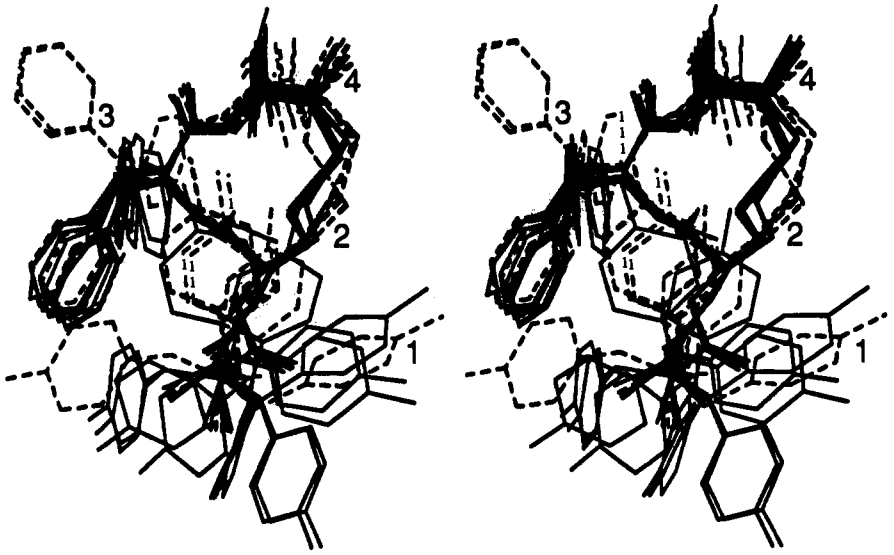

Figure 1. Superposition (stereoview) of 20 JOM-13 conformers with relative energies $\Delta E < 3$ kcal/mol. Conformers with χ^1 angle of Cys^2 $\approx$180° are indicated by dashed line. C$^\alpha$ atoms of the Tyr^1, *D*-Cys^2, and Phe^3 residues were used for superposition.

conformational information for the peptide ligand (either in solution or solid state) in the absence of receptor can be obtained, and insight into the possible receptor-bound conformation of the peptide derives only from the extrapolation of this free ligand information. For such extrapolations to be realistic, the conformation of this peptide ligand should be relatively environment independent, which will be realized only if the ligand exhibits reduced conformational lability compared to the linear and highly flexible native ligands.

One enkephalin analog designed with this criterion in mind is the cyclic pentapeptide DPDPE, Tyr-*cyclo*[D-Pen-Gly-Phe-D-Pen]OH (where Pen, penicillamine, is β,β-dimethylcysteine), which we described several years ago.[2] This analog, which is conformationally constrained due to the cyclization *via* a disulfide bond between the side chains of residues 2 and 5 and is further restricted by the rigidizing effect of the *gem*-disubstituted Pen residues, displays very high selectivity for the δ-type of opioid receptor and thus represents a tool for the elucidation of the active conformation required at this receptor type. Reports from our lab[3] and others[4-10] have proposed disparate models for the solution and/or active conformation of DPDPE. The discrepancies among these several different models for DPDPE conformation suggest that even though DPDPE is conformationally restricted, it still possesses significant residual flexibility. Consequently, many low-energy conformers are accessible, leading to different proposed models based upon molecular mechanics calculations using different force fields or conformational search strategies. As with flexible, linear peptides, the residual dynamic averaging in a flexible DPDPE would also result in unrealistic interproton distances inferred from NOE measurements reflecting an average, rather than a unique conformation. Sources of this flexibility in DPDPE include the relatively unhindered exocyclic Tyr residue, the Phe side chains, and the central Gly residue, which, lacking a side chain, can assume many low-energy backbone conformations. In an attempt to address this last source of flexibility, we investigated a series of des-Gly^3 analogs of DPDPE. In the resulting more rigid cyclic tetrapeptide series, the analog Tyr-*cyclo*[D-Cys-Phe-D-Pen]OH (JOM-13), in which the disulfide bond forms an 11-membered ring *vs* the 14-membered cycle in DPDPE, was shown to exhibit δ binding affinity and selectivity similar to those of DPDPE.[11] ^{1}H NMR studies in aqueous solution revealed that this tetrapeptide exists in two distinct conformations on the NMR time scale, as evidenced by two sets of resonances.[12] Large differences in the observed chemical shifts and coupling constants for the D-Cys^2 residue in the two conformers suggested that the major differences between the two NMR conformers reside in the disulfide portion of the molecule; however, a paucity of conformationally informative NOE interactions precluded the development of a detailed structural model from the NMR studies.

In the present study we report the results of an X-ray crystallographic study and theoretical conformational analysis of JOM-13. Comparison of the computational, X-ray solid state, and ^{1}H NMR solution conformational features reveals a striking degree of similarity, particularly in the cyclic portion of the molecule, confirming that this 11-membered ring in JOM-13 possesses well-defined conformational features. The high affinity displayed by this analog for the δ opioid receptor derives from the ability of this relatively rigid, cyclic scaffolding to maintain δ receptor-preferring orientations among the presumed pharmacophoric elements, the exocyclic Tyr amino and phenolic functions and the Phe aromatic side chain.

Results

Molecular Mechanics Simulations. The 20 lowest-energy conformers of JOM-13, with relative energies $\Delta E < 3.0$ kcal/mol, are chosen to represent results of the molecular mechanics computations (see Experimental Section) for JOM-13 using the QUANTA 3.3/CHARMm force field (Figure 1 and Table 1). All 20 conformers have almost identical main-chain torsion angles within the disulfide-containing, 11-membered cycle formed by the C-terminal tripeptide D-Cys-Phe-D-Pen (the angles ψ of D-Cys^2, ϕ and ψ of Phe^3, and ϕ of D-Pen^4 in Table 1) but may

(2) Mosberg, H. I.; Hurst, R.; Hruby, V. J.; Gee, K.; Yamamura, H. I.; Galligan, J. J.; Burks, T. F. *Proc. Natl. Acad. Sci. U.S.A.* **1983**, *80*, 5871–5874.
(3) Mosberg, H. I.; Sobczyk-Kojiro, K.; Subramanian, P.; Crippen, G. M.; Ramalingam, K.; Woodard, R. W. *J. Am. Chem. Soc.* **1990**, *112*, 822–829.
(4) Hruby, V. J.; Kao, L.-F.; Pettitt, B. M.; Karplus, M. *J. Am. Chem. Soc.* **1988**, *110*, 3351–3359.
(5) Pettitt, B. M.; Matsunaga, T.; Al-Obeidi, F.; Gehrig, C.; Hruby, V. J.; Karplus, M. *Biophys. J.* **1991**, *60*, 1540–1544.
(6) Froimowitz, M. *Biopolymers* **1990**, *30*, 1011–1025.
(7) Chew, C.; Villar, H.; Loew, G. *Mol. Pharmacol.* **1991**, *39*, 502–510.
(8) Smith, P.; Pettitt, B. *J. Am. Chem. Soc.* **1991**, *113*, 6029–6037.
(9) Wilkes, B.; Schiller, P. *J. Comput.-Aided Mol. Des.* **1991**, *5*, 293–302.
(10) Nikiforovich, G. V.; Golbraikh, A. A.; Shenderovich, M. D.; Balodis, J. *Int. J. Pept. Protein Res.* **1990**, *36*, 209–218.
(11) Mosberg, H. I.; Omnaas, J. R.; Smith, C. B.; Medzihradsky, F. *Life Sci.* **1988**, *43*, 1013–1020.
(12) Mosberg, H. I.; Sobczyk-Kojiro, K. In *Proteins*; Renugopalakrishnan, V., Ed.; ESCOM: Leiden, the Netherlands, 1991; pp 105–109.
(13) Shenderovich, M. D., Nikiforovich, G. V., Golbraikh, A. A. *Int. J. Pept. Protein Res.* **1991**, *37*, 241–251.
(14) Nikiforovich, G. V.; Hruby, V. J.; Prakash, O.; Gehrig, C. A. *Biopolymers* **1991**, *31*, 941–955.

Table 1. Torsion Angles (deg) of JOM-13 Low-Energy Computed Conformations (average values ± rms deviations for the families A, B, and C), the Crystal Conformers A_C and B_C (± estimated standard deviations from least-squares refinement), and Lowest Energy Conformers of JOM-13 from Previous Computations (refs 13 and 14)

	structure					from ref 13	from ref 14
	A	A_C	B	B_C	C		
N^a	13		5		2		
$\Delta E_{min}{}^b$	0.1		0.0		1.3		
D-Cys^2 χ^1	−57 ± 2	−51 ± 1	178 ± 2	165 ± 1	178 ± 2	176	168
D-Cys^2 χ^2	−148 ± 1	−141 ± 1	150 ± 4	144 ± 1	71 ± 1	*c*	*c*
D-Cys^2 χ^3 (S–S)	93 ± 1	89 ± 1	−103 ± 1	−99 ± 1	87 ± 1	*c*	79
D-Pen^4 χ^1	−71 ± 1	−76 ± 1	−70 ± 1	−72 ± 1	48 ± 2	−62	46
D-Pen^4 χ^2	52 ± 1	50 ± 1	91 ± 5	89 ± 1	−143 ± 1	*c*	*c*
Tyr^1 ψ	153 ± 13 −77 ± 1	159 ± 1	141 ± 8 −56^d	102 ± 1	143 ± 6	157	150
Tyr^1 ω	181 ± 2	177 ± 1	179 ± 1	−175 ± 1	176 ± 1		
D-Cys^2 φ	157 ± 5 75 ± 5	136 ± 1	160 ± 5 85 ± 9	67 ± 1	166 ± 2	166	76
D-Cys^2 ψ	36 ± 3	18 ± 1	48 ± 2	44 ± 1	46 ± 1	54	50
D-Cys^2 ω	171 ± 1	166 ± 1	166 ± 3	162 ± 1	177 ± 1		
Phe^3 φ	−83 ± 3	−84 ± 1	−83 ± 4	−63 ± 1	−79 ± 5	−80	−77
Phe^3 ψ	−38 ± 4	−15 ± 1	−24 ± 5	−31 ± 1	−49 ± 5	−30	−38
Phe^3 ω	174 ± 1	165 ± 1	−178 ± 3	−174 ± 1	168 ± 1		
D-Pen^4 φ	138 ± 2	133 ± 1	138 ± 1	138 ± 1	131 ± 1	136	124

^{a} N is the number of conformations, in each family, with relative energy $\Delta E < 3$ kcal/mol. ^{b} ΔE_{min} is the relative energy (kcal/mol) of the lowest energy conformer in the given family. ^{c} These torsion angles were not reported in refs 13 and 14. ^{d} This set of angles was represented by a single conformation of JOM-13 within the energy interval 0–3.0 kcal/mol.

be readily classified into three different families, A, B, and C, which differ in the geometry of the disulfide bridge (the χ^1, χ^2, and χ^3 angles of the D-Cys^2 and D-Pen^4 residu es). Structures A and B differ mainly in angles χ^1 and χ^3 (i.e., around the S–S bond) of the D-Cys^2 residue, while structures B and C have the same D-Cys^2 χ^1 angle but differ in all other torsion angles of the disulfide bridge (see Table 1). All torsion angles ϕ and ψ of all the low-energy conformers are within allowed regions of the Ramachandran plot.

As is evident from Figure 1, some elements of the JOM-13 spatial structure retain considerable flexibility. First, the side chains of both the Tyr^1 and Phe^3 residues may assume *trans*, *gauche*$^+$, or *gauche*$^-$ conformations. Second, two local minima of energy arise for the Tyr^1 ψ angle (~145° and −65°, see Table 1) as well as two minima for the angle ϕ of the D-Cys^2 residue (~80° and 160°). Consequently, the first peptide group between the Tyr^1 and D-Cys^2 residues may assume several different orientations (see Figure 1). Third, as has been noted, the S–S bridge has three different configurations corresponding to conformer families A, B, and C. It is important to note that all these flexible elements (Tyr^1 and Phe^3 side chains, first peptide group, and S–S bridge) can be varied almost independently of each other and have no influence on the main-chain structure within the tripeptide cycle. Intramolecular hydrogen bonding is absent throughout the series of low-energy JOM-13 conformers, with the exception of a hydrogen bond between the Tyr^1 O$^\zeta$H and the D-Pen^4-COO$^-$ observed for some orientations of the Tyr side chain.

Crystal Structure. The results of the X-ray study are shown in Figure 2. There are two independent peptide molecules, A_C (residues 1–4) and B_C (residues 5–8), and six molecules of water in the asymmetric unit. There are a total of four peptide molecules, A_C, A_C', B_C, and B_C', within the unit cell. The A_C and B_C molecules are related to the corresponding, identical A_C' and B_C' molecules by a crystallographic 2-fold axis. The distance between the two aromatic ring centers in the individual molecules is 10.9 Å in A_C and 13.6 Å in B_C. However, the aromatic rings in the Tyr side chains for the two molecules in the asymmetric unit are only 4.7 Å apart. There are no intramolecular hydrogen bonds; however, there is an extensive system of peptide–peptide, peptide–water, and water–water intermolecular hydrogen bonds which influence the 3-dimensional packing of the peptide molecules (Figures 3 and 4). All possible peptide hydrogen donors, except N-H of D-Pen^4 and D-Pen^8, are involved in the hydrogen-bonded network, as are all possible acceptors, except for O$^\zeta$ of the Tyr side chain of molecule B_C. All intermolecular peptide–peptide hydrogen bonds are of the $A_C\cdots B_C$ type. There are no $A_C\cdots A_C'$ or $B_C\cdots B_C'$ interactions.

Molecule A_C forms three A_C—H···B_C hydrogen bonds, and molecule B_C forms five B_C—H···A_C hydrogen bonds (see Figures 3 and Table 2). Seven of these bonds have the effect of linking the peptide molecules into columns that are two molecules wide. Each column is formed by translating molecules A_C and B_C (see molecules A-1, B-1, A, and B in Figure 3). The A_C–$(B'-1)_C$ pair of molecules that gives the column its width is arranged such that the 11-membered rings nearly line up with one another within a column but are rotated by 180° such that the S–S bonds lie on the same side of the column and nearly eclipse one another. The hydrogen bonds link molecules along and across the column, but there are no links to other identical columns related by simple unit cell translations. The carbonyl oxygens not involved in peptide–peptide interactions are oriented such that they interact with water molecules coming between the peptide molecules along the column (see Figure 4). All the Tyr side chains are on one side of the column with the Phe side chains on the opposite side of the column. The planes through the Tyr rings are approximately parallel to one another (angle between the planes = 21.7°).

The column consisting of molecules $(A-1)_C$, $(B-1)_C$, A_C, and B_C is related to that formed by molecules $(A-1)_C'$, $(B-1)_C'$, A_C', and B_C' by a crystallographic 2-fold screw axis along the *b* cell direction. These columns are connected by an additional peptide–peptide hydrogen bond in which O$^\zeta$H of Tyr^5 in molecule B_C acts as a donor to the –C=O oxygen of D-Cys^2 in molecule A_C, see Figure 3). The closest $A_C\cdots A_C'$ approaches are between these symmetry-related columns and involve water bridges linking O$^\zeta$ of Tyr^1 with –C=O of Phe^3 and –C—O$^-$ of D-Pen^4 (see Figure 4). Except for interactions listed in Table 2, there are no intermolecular approaches less than van der Waals separations.

Discussion

Structure of the Tripeptide Cycle. The combined use of theoretical and experimental approaches in peptide conformational analysis has obvious advantages. While X-ray analysis

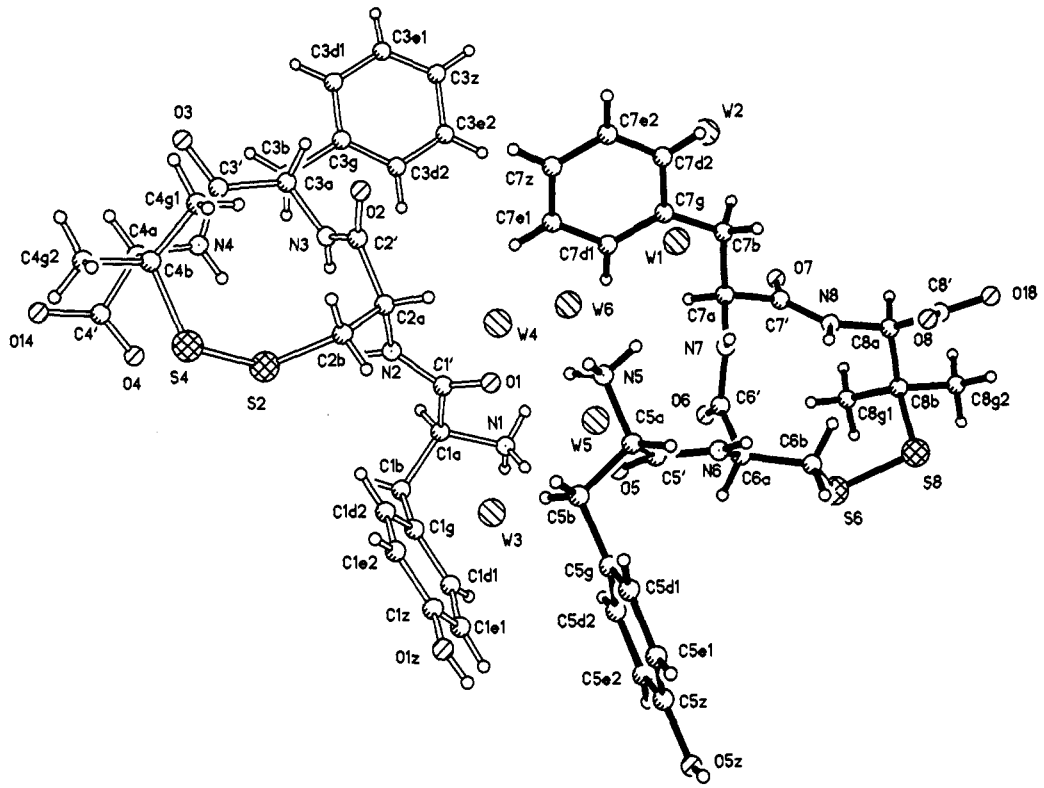

Figure 2. Results of the X-ray analysis of JOM-13. The figure has been drawn using the experimentally determined coordinates with the thermal ellipsoids at the 20% probability level.

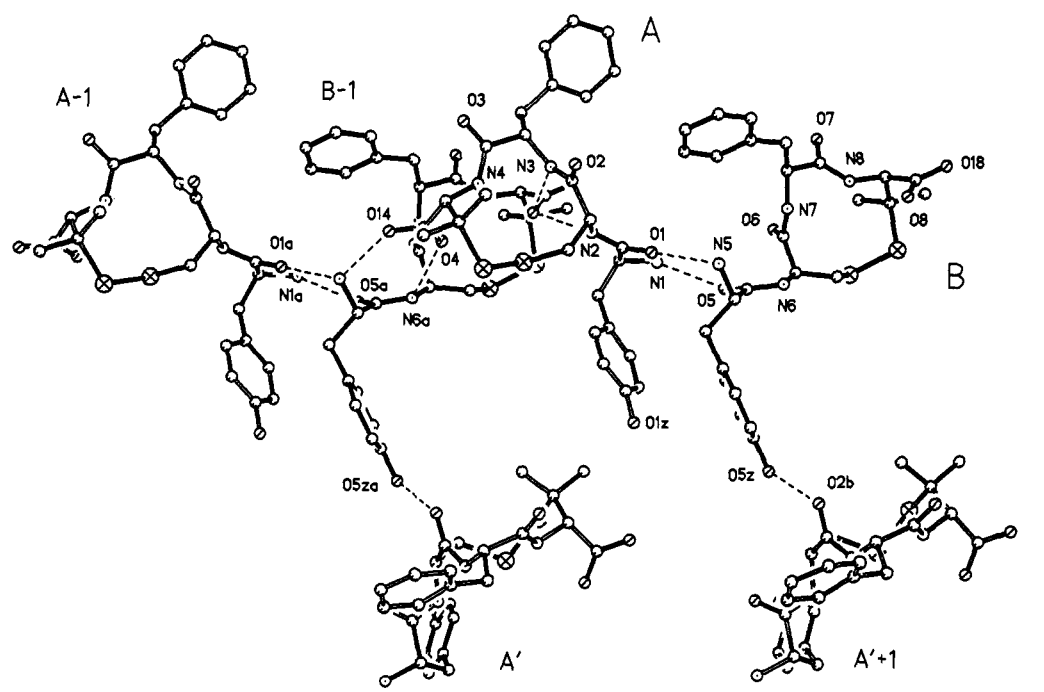

Figure 3. Peptide–peptide hydrogen-bonding scheme. The H-bonds linking molecules along and across individual columns are shown, as is the single peptide–peptide H-bond linking columns related by the crystallographic 2-fold axis (*A* and *A'*). The minimum number of molecules of JOM-13 necessary to indicate all unique hydrogen bonds are shown.

and NMR spectroscopy allow the determination of a few conformations of a peptide, which are stable under defined experimental conditions in solution and crystalline environments, a different conformation may be stabilized by interactions of the peptide with the receptor binding site. Therefore, a large set of alternative structures should be simulated by molecular mechanics or dynamics methods in the search for biologically active peptide conformations. At the same time, this theoretically generated set should be compared with experimental data to verify the reliability of the computational results and to analyze the dependence of the peptide structure on its environment. Unlike short, linear peptides and cyclic peptides containing large cycles, which tend to display considerable flexibility, the conformation of the 11-membered, disulfide-containing ring of JOM-13 and its analogs is expected to be determined mainly by the steric and covalent constraints within the ring which do not depend on environment. JOM-13 then represents a good model for the elaboration of the active conformation at δ opioid receptors based

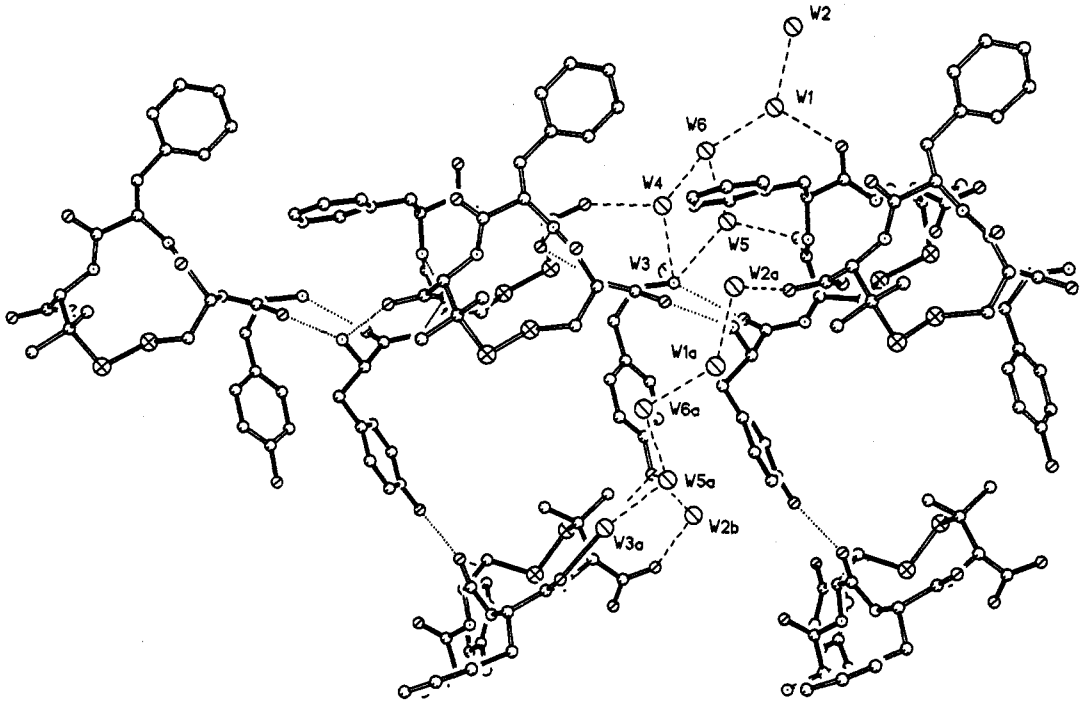

Figure 4. Several water molecules have been added to the peptide molecules shown in Figure 3 to illustrate the peptide–water and water–water hydrogen-bonding scheme. The water molecules are distributed between peptide molecules along but not across individual columns. There are also water bridges which provide additional links to symmetry-related columns.

Table 2. Hydrogen Bond Parameters for JOM-13

donor	acceptor	symmetry	N···O O···O	H···O	N—H···O O—H···O
		Molecule A			
N1	W4		2.921	2.239	133.1
N1	W3		2.699	1.814	172.7
N1	O5		2.901	2.176	138.2
N2	O8	$x, y, -1 + z$	2.831	1.985	167.7
N3	O8	$x, y, -1 + z$	2.853	2.065	152.0
N4	none				
O$^{\zeta}$1	W2	$1 - x, 0.5 + y, 1 - z$	2.670	1.880	161.6
		Molecule B			
N5	O14	$x, y, 1 + z$	2.704	1.903	148.9
N5	W1	$1 - x, y, z$	2.796	1.923	166.6
N5	O1		2.791	1.918	166.7
N6	O4	$x, y, 1 + z$	2.965	2.514	113.6
N7	O4	$x, y, 1 + z$	2.840	2.053	151.9
N8	none				
O$^{\zeta}$5	O2	$2 - x, 0.5 + y, 1 - z$	2.782	2.041	150.2
		Solvent			
W1	O7		2.690		
W1	W6		2.912		
W2	O14	$-1 + x, y, 1 + z$	2.706		
W2	W1		2.912		
W3	O$^{\zeta}$1	$-1 + x, y, z$	2.834		
W3	O3	$2 - x, 0.5 + y, -z$	2.651		
W4	O18	$x, y, -1 + z$	2.730		
W4	W6		2.738		
W5	O6		2.726		
W5	O$^{\zeta}$1	$-1 + x, y, z$	2.969		
W6	W5		2.846		
		Other Approachers < 3.2 Å			
N1	W5		3.184		
W3	W5		3.129		

on the comparison of theoretical and experimental solution- and solid-state results for the ligand in the absence of the receptor. Indeed, all experimental (i.e., solution NMR and X-ray crystallography) and computational studies of JOM-13 show the existence of the same two cyclic structures of the peptide.

As we have previously reported, two distinct sets of proton signals are observed in the ^{1}H NMR spectrum of JOM-13 in aqueous solution,[12] indicative of two slowly exchangeable structures, I and II. The relative occupancies of conformers I and II were estimated from NMR signal intensities as 68:32, which corresponds to an energy difference, ΔE, of only ~0.5 kcal/mol. As previously pointed out,[12] the major differences in the proton chemical shifts and coupling constants of conformers I and II are confined to the D-Cys^2 and D-Pen^4 residues, suggesting that conformers I and II differ primarily in the region of the disulfide. The observed vicinal coupling constants for the two conformers, summarized in Table 3, confirm this interpretation. The measured values for the vicinal coupling constants for the D-Cys^2 protons H-C$^{\alpha}$C$^{\beta}$-H and H-C$^{\alpha}$C$^{\beta'}$-H for structure I (3.0 and 3.0 Hz, i.e., both β-protons in a *gauche* orientation relative to the α-proton) indicate that the preferred side-chain rotamer for this conformer should have $\chi^1 \approx -60°$, while the coupling constants observed for conformer II (13.0 and 2.5 Hz, i.e., one β-proton *trans* to the α-proton, the other *gauche*) c orrespond to $\chi^1 \approx +60°$ or 180°.

The calculated cyclic structures, A and B, of JOM-13 have exactly the same values of the D-Cys^2 χ^1 angle (about –60° and about 180°, respectively, see Table 1) as would be predicted from the NMR data for conformers I and II, respectively. Further, within the rigid 11-membered ring of JOM-13, all theoretically calculated vicinal coupling constants for main- and side-chain protons in both structures A and B are in good agreement (differences < 1 Hz) with those observed in the NMR experiments (Table 3). Consequently, NMR structures I and II can be represented by the computational conformational families, A and B, respectively. The observation of large differences in chemical shifts for the C$^{\alpha}$H proton of D-Cys^2 (0.60 ppm) in NMR conformers I and II is also consistent with this assignment and may be explained by the different positions in the corresponding computed structures A and B of the D-Cys^2 S$^{\gamma}$ atom which forms van der Waals contacts with this proton in structure B. The resulting increase in electronic shielding is consistent with the observed upfield shift of this resonance in conformer II.[12] The absence, in the NMR spectrum, of the third low-energy structure

(15) Bystrov, V. F. *Prog. NMR Spectrosc.* **1976**, *10*, 41–81.
(16) Cung, M. T.; Marraud, M. *Biopolymers* **1982**, *21*, 953–967.

Table 3. Experimental ($^3J^{exp}$) and Calculated ($^3J^{clc}$) Vicinal Coupling Constants (Hz) for Structures A and B of JOM-13

		$^3J^{exp}$		$\langle ^3J^{clc}(\theta^{clc})\rangle^a$		$^3J^{clc}(\theta^{X\text{-}ray})^b$	
vicinal protons	residue	A	B	A	B	A	B
H-NC$^\alpha$-H	D-Cys^2	10.0	5.5	6.0–6.1	6.3–6.5	9.3	4.1
H-NC$^\alpha$-H	Phe^3	5.5	5.5	6.3–6.5	6.4–6.6	6.6	3.5
H-NC$^\alpha$-H	D-Pen^4	8.0	7.5	8.5–9.2	8.4–9.1	9.5	9.1
H-C$^\alpha$C$^\beta$-H	D-Cys^2	3.0	13.0	3.9–4.3	12.9–13.9	5.0	12.9
H-C$^\alpha$C$^{\beta'}$-H	D-Cys^2	3.0	2.5	3.2–3.8	2.0–3.3	2.5	2.0

^{a} The average vicinal coupling constants, $\langle ^3J^{clc}(\theta^{clc})\rangle$, were calculated for the final set of 20 JOM-13 conformations with $\Delta E < 3$ kcal/mol, which were considered to be equally populated:

$$\langle ^3J^{clc}(\theta^{clc})\rangle = \frac{1}{N}\sum_{i=1}^{N} {}^3J^{clc}(\theta_i)$$

$$^3J^{clc}(\theta_i) = a\cos^2\theta_i + b\cos\theta_i + c$$

where N is the number of conformations in the set A or B; θ_i is the dihedral angle, H–X–Y–H, in the ith conformation; and a, b, and c are coefficients from refs 15 and 16 for vicinal coupling constants of protons H-NC$^\alpha$-H and H-C$^\alpha$C$^\beta$-H, respectively. The interval of $\langle ^3J^{clc}(\theta^{clc})\rangle$ values reflects differences between averaging within the low-energy set of vicinal coupling constants, $^3J^{clc}(\theta_i)$, that are "fixed" or additionally "locally averaged" within each conformation. The "local averaging" of $^3J^{clc}(\theta_i)$ was done assuming equal occupancy in the interval $[\theta_i - 30°; \theta_i + 30°]$ in each conformation. ^{b} The $J^{clc}(\theta^{X\text{-}ray})$ constants were calculated directly from crystallographic structures A and B.

(C, ΔE_{min} = 1.1 kcal/mol, see Table 1) may be due to its relatively low statistical weight. Each structure (A, B, and C) is represented by a number (N in Table 1) of low-energy conformations which differ in the orientations of the exocyclic Tyr residue and the Phe side chain. The greater representation of structure A in the set of low-energy conformations (N_A = 13 *vs* N_B = 5 in Table 1) is in agreement with its higher occupancy (68:32) in solution as detected by ^{1}H NMR spectroscopy.[12]

The X-ray diffraction study reveals two independent conformers in the unit cell, A_C and B_C (Figure 2). Conformations of the tripeptide cyclic fragment, including the disulfide bridge, for A_C and B_C are almost identical to corresponding calculated conformations of JOM-13 for families A and B, respectively. The differences in torsion angles are less than 10°, except for ψ of D-Cys^2 and Phe^3 (A *vs* A_C) and for ϕ of Phe^3 (B *vs* B_C) in which torsion angle differences are ~20° (see Table 1). Root mean square deviations of main-chain atomic coordinates within the cycle are always <0.3 Å (0.2 Å on average) between the calculated and crystal conformations, <0.2 Å (0.1 Å on average) within the calculated set of 20 low-energy conformations, and 0.21 Å between the two independent crystal conformations, A_C and B_C. To directly compare the crystal structures of JOM-13 with the NMR solution data, the values of the vicinal coupling constants were calculated for the X-ray torsion angles. These values, presented in Table 3, are also in excellent agreement with the experimental ones.

The conformational transition between conformers A and B may be described as the simultaneous change of the C$^\beta$–S–S–C$^\beta$ and D-Cys^2 χ^1 torsion angles from +93 to −103° and from −57° to 178°, respectively (Table 1). This transition, which requires concerted motions within the small tripeptide ring structure, is slow on the NMR time scale, giving rise to the observed two sets of resonances. The energy barrier between the two structures is lower if the size of the cycle is increased. For instance, for JOM-13 analogs in which the S–S bond is replaced by the S–$(CH_2)_n$–S group (n = 1, 2, 3), only a single set of NMR signals is observed, due to the faster conformational interconversions in the larger dithioether-containing rings.[17] Similarly, for DPDPE, in which the cycle size is increased by incorporating a glycine residue between the sulfur-containing amino acids, only a single set of NMR signals is observed. The computational results clearly indicate that the tripeptide cycle of JOM-13 is more rigid than the corresponding tetrapeptide cycle of DPDPE; 24 different ring structures of DPDPE within the same energy interval 0–3 kcal/mol (compared to the three JOM-13 structures, A, B, and C) have been observed in a similar theoretical conformational analysis.[6]

It is interesting to compare our data with previous results of JOM-13 computations employing the ECEPP/2 force field.[13,14] The common lowest-energy backbone structure within the tripeptide cycle found in A and B was also observed in the earlier studies (see torsion angles ψ of D-Cys^2, ϕ and ψ of Phe^3, and ϕ of D-Pen^4 in Table 1). However, the main conformer of the S–S bridge with χ^1 of D-Cys^2 ≈ −60° (i.e., structure A) was not represented within the set of structures with energies < 10 kcal/mol reported by Shenderovich *et al.*[13] and was obtained by Nikiforovich *et al.*[14] only in combination with higher-energy main-chain structures of the tripeptide cycle. A comparison of torsion angles in Table 1 shows that the lowest-energy conformations proposed by Shenderovich *et al.*[13] and by Nikiforovich *et al.*[14] correspond to the cycle structures B and C, respectively (Structure C was also represented in ref 13 with relative energy = 4.9 kcal/mol). All other conformations described by Nikiforovich and co-workers[13,14] differ from the crystallographic ones and have relative energies > 3 kcal/mol after their optimization with the CHARMm force field. The omission in previous computations of the main conformer, A, of JOM-13 reported here is probably attributable to energy minimization of the short, strained, 11-membered ring of JOM-13 in the space of torsion angles (ECEPP/2 force field) compared with minimization in atomic coordinate space (CHARMm). Conformer A and all other ring structures of JOM-13 reported here were reproduced correctly with the ECEPP/2 force field when "soft" disulfide bond closing functions (see Experimental Section) were used. However, in this case some improper distortions of the S–S bridge geometry are allowed (up to 0.2–0.3 Å in terms of interatomic distances).

Flexible Elements of JOM-13. All experimental and computational data indicate that, unlike the cyclic part of the molecule, all exocyclic elements (i.e., the Tyr^1 residue and Phe^3 side chain) are flexible. The measured vicinal coupling constants of Tyr^1 and Phe^3 side-chain protons H-C$^\alpha$C$^\beta$-H are in the range of 6.5–9.0 Hz,[12] consistent with dynamic averaging. All *trans*, *gauche*$^+$, and *gauche*$^-$ rotamers of Tyr^1 and Phe^3 side chains are represented in the set of JOM-13 low-energy conformations (Figure 1). These two side chains have different orientations in crystal conformers A_C and B_C (Figure 2); the χ^1,χ^2 angles of Tyr^1 are 70°,84° and −170°,−90°, and the χ^1,χ^2 angles of Phe^3 are −83°, 76° and −68°,−14° in conformations A_C and B_C, respectively.

In addition to the side chains, the first peptide group (between Tyr^1 and D-Cys^2) may also assume different conformations because of the existence of two local energy minima for both the ψ angle of the Tyr^1 and the ϕ of the D-Cys^2 residues ($\psi \approx 145°$ and −65°; $\phi \approx 80°$ and 160°, see Table 1). All four combinations of these local minima are possible. This leads to a variety of orientations of the entire Tyr^1 residue relative to the rest of the molecule (Figure 1). Two of these orientations are realized in molecules A_C and B_C from the X-ray study (Figure 2). However, unlike the cyclic part of the JOM-13 molecule, the conformations of its flexible elements are stabilized mainly by intermolecular packing forces in the crystalline environment (especially interactions of molecule A_C with $(B\text{-}1)_C$ and B_C (Figures 2–4)), including a network of intermolecular hydrogen bonds and electrostatic and van der Waals interactions. Energy minimization of X-ray conformers A_C and B_C leads to slightly different conformations which differ mainly in the exocyclic angles, ϕ of D-Cys^2 and χ^1,χ^2 of Tyr^1 and Phe^3 residues (Figure 5). These latter conformers are identical to members of the set of calculated low-energy JOM-13 conformations (Figure 1) and have relative energies 2.6 and 2.4 kcal/mol, respectively.

(17) Sobczyk-Kojiro, K.; Mosberg, H. I., unpublished observations.

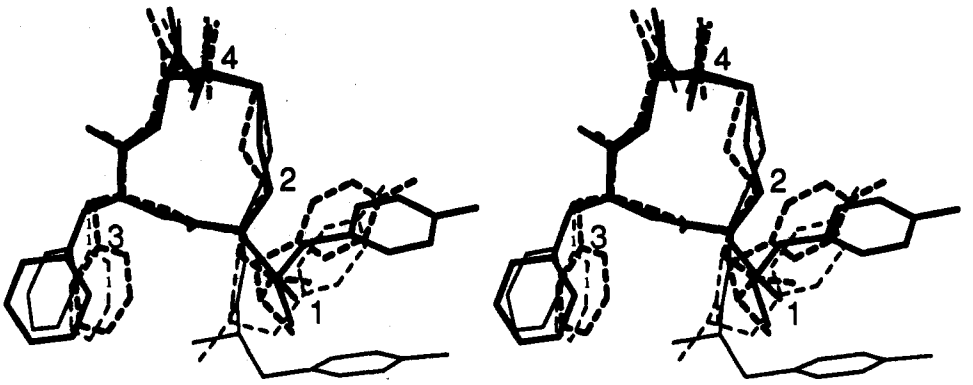

Figure 5. Stereoview of crystal conformers A_C and B_C (bold line) and the corresponding energy-minimized conformers (thin line) of JOM-13. Side chains are numbered according to primary sequence.

Dynamic averaging effects near the first peptide group are obvious also from the comparison of calculated and observed values of the D-Cys[2] H-NC$^{\alpha}$-H vicinal coupling constant. Two different conformers of equal energy for this residue (with $\phi \approx$ 160° and 80°, see Table 1) are separated by a small energy barrier (~3 kcal/mol using the CHARMm force field). Both values of ϕ (i.e., 160° and 80°) correspond to the same vicinal coupling constant (~6 Hz) for the H-NC$^{\alpha}$-H protons, which is in agreement with the NMR experimental value for structure B (5.5 Hz, Table 3). For structure A, however, this constant was determined experimentally to be 10 Hz, which corresponds to a ϕ angle (~120°) intermediate between the two local minima of energy and closer to the angle observed in crystal conformation A_C (136°, Table 1). A better fit between the theoretical and experimental values for this coupling constant results if a continuous set of structures in the interval of ϕ = 80°–160° is averaged instead of only those conformations that correspond to the local energy minima. For example, the calculated value for this coupling constant is 8.6 Hz if equally populated values of ϕ within the interval 80°–160° are assumed, in better agreement with the experimental value.

Conclusions

The results presented here provide clear evidence that the conformationally restricted, 11-membered ring of JOM-13 serves as an environment-independent structural framework and that, consequently, the conformational analysis of JOM-13 and its analogs in the absence of opioid receptor is a viable approach toward the elucidation of the bioactive, receptor-bound conformation. In this regard, JOM-13 provides distinct advantages over the pentapeptide DPDPE, in which the larger 14-membered cycle gives rise to many more low-energy ring structures. However, despite the conformational rigidity of the JOM-13 cyclic scaffold, considerable conformational lability exists for precisely those elements, the Tyr amino and phenolic functions, and the Phe aromatic side chain, which are required for bioactivity. Also unanswered in the present study is whether only one (and if so, which) of the observed conformational families is compatible with δ opioid activity. Accordingly, the results presented here are insufficient for the development of a realistic, detailed model of the δ receptor pharmacophore. This should be appreciated as being the general case for the conformational analysis of conformationally restricted peptides since significant residual flexibility of the pharmacophoric elements is a common design feature of such analogs. Development of a reliable model for the bioactive conformation then requires the additional design, synthesis, and evaluation of analogs in which conformational constraints are also incorporated into the pharmacophoric elements. Several such analogs, in which different, limited regions of conformational space are allowed for each of these structural elements, must be compared and the conformational features correlated with bioactivity data before a realistic model can be proposed. These types of studies utilizing the conformationally well-defined 11-membered cycle of JOM-13 as the scaffold are in progress in our laboratory.

Experimental Section

Crystallization. The stock solution (18.5 mg/mL in water) of JOM-13 was filtered by centrifugation for 5 min through a Millipore Ultrafree μC Durapore 0.22-μm filter and stored at room temperature. A vapor diffusion technique[18,19] using hanging drops suspended from silinated glass coverslips sealed over wells of Linbro tissue culture plates was used for crystallization trials with Hampton screen kit HR-CS1 (Hampton Research, Riverside, CA). Tiny crystals were obtained in the droplet containing 5 μL of stock peptide solution and 5 μL of reservior solution against 500-μL reseroirs containing 0.2 M ammonium sulfate, 0.1 M sodium acetate (pH 4.6), and 30% w/v PEG 4000. Diffraction-sized crystals were grown, over a 5–15 day period, from 30-μL sitting drops initially containing equal volumes of stock solution and reservior solution. A constant temperature of 22 °C was maintained in a Napco Model 2900 incubator for all the crystallization experiments.

X-ray Diffraction. The data crystal was selected from the sitting drop and coated with microscope immersion oil (Cargille Type NVH). The coated crystal was mounted on a thin glass rod and transferred immediately into a –40 °C nitrogen stream for data collection on an automated four-circle diffractometer (Siemens R3m/V) equipped with an incident beam graphite monochromator. Cell dimensions were determined by a least-squares fit to the experimentally determined positions for 25 high-angle reflections (2θ values between 62° and 81°). Three reflections, used as standards, were remeasured after every 97 new measurements and showed random fluctuations of ±2.5%. The data were corrected for Lorentz and polarization effects, and a face-indexed numerical absorption correction was applied. The structure was solved by direct methods with the aid of the program SHELX86[20] and refined on F_o^2 values using the full-matrix least-squares program SHELXL-93.[21] Refining on F_o^2 values, as opposed to conventional refinement on F_o values, allows all data to be used rather than just data with F_o greater than a specified threshold. As a result, the experimental information is more fully exploited, which can appreciably improve the precision of the structure determination. The resulting R-factor, w$R2$, is for statistical reasons about twice as large as the conventional F_o-based R-factor, $R1$. R values are listed in Table 4 along with other pertinent experimental data including the estimated Flack "racemic twinning parameter" which is calculated as a check on whether or not the experimental data are accurate enough to determine the absolute configuration.[22] A value of 0.0 for the Flack parameter indicates the correct choice (a value of 1.0 indicates the incorrect hand). For JOM-13, 741 parameters were refined which included atomic coordinates and anisotropic thermal parameters for all non-hydrogen

(18) McPherson, A. *Preparation and Analysis of Protein Crystals*; John Wiley & Sons: New York, 1982; p 96.
(19) Ducruix, A.; Giege, R. In *Crystallization of Nucleic Acids and Proteins: A Practical Approach*; Ducruix, A., Giege, R., Eds.; Oxford Univ. Press: New York, 1992; pp 73–98.
(20) Sheldrick, G. M. *SHELX86, Program for the solution of crystal structures*; Univ. of Gottingen: Federal Republic of Germany, 1986.
(21) Sheldrick, G. M. *J. Appl. Cryst.*, submitted.
(22) Flack, H. D. *Acta Crystallogr.* **1983**, *A39*, 876–881.

Table 4. Crystal Data and Structure Refinement Parameters

Crystal Data	
empirical formula	$C_{26}H_{32}N_4O_6S_2 \cdot 3H_2O$
crystal habit	clear colorless plates
crystal size	0.60 × 0.36 × 0.16 mm³
crystal system	monoclinic
space group	$P2_1$
unit cell dimensions	a = 10.610(3) Å, α = 90°
	b = 21.382(5) Å, β = 99.14(2)°
	c = 13.554(4) Å, γ = 90°
volume	3035.9(14) Å³
Z	4
density (calculated)	1.345 Mg/m³
absorption coefficient	2.073 mm⁻¹
formula weight/F(000)	614.72/1304
Data Collection	
wavelength/temperature	1.54178 Å/253(2) K
scan type	$\theta/2\theta$
scan speed	variable depending upon intensity
index ranges	$-11 \le h \le 11, 0 \le k \le 22, 0 \le l \le 14$
reflections collected	4435
independent reflections	4093 (R_{int} = 0.040 00)
observed reflections	3876 [$I > 2\sigma(I)$]
resolution	0.93 Å
absorption correction	FACE indexed numerical
max and min transmission	0.712 and 0.332
Refinement	
refinement method	full-matrix least-squares on F^2
data/restraints/parameters	4093/1/741
goodness-of-fit on F^2	1.030
final R indices [$I > 2\sigma(I)$]	$R1$ = 0.0699, w$R2$ = 0.1851
R indices (all data)	$R1$ = 0.0722, w$R2$ = 0.1890
absolute structure parameter	0.03(3)
extinction coefficient	0.0023(5)
largest diff peak and hole	1.224 and −0.483 eÅ⁻³

atoms. Hydrogen atoms on the peptide molecules were included using a restrained riding model with thermal parameters set to be equal to either $1.1U_{eq}$ (for NH, CH, and CH_2 groups) or $1.2U_{eq}$ (for CH_3 and HO) of their covalently bonded atoms. All coordinates, including H atoms, have been deposited with the Cambridge Crystallographic Data Centre, Cambridge University Chemical Laboratory, Cambridge CB2 1EW, England.

Molecular Mechanics Calculations. The search for low-energy conformations of JOM-13 was done in two stages. First, the set of low-energy conformers of the cyclic fragment CH_3CO-*cyclo*[D-Cys-Ala-D-Pen]OH was calculated. Second, these conformers of the cyclic fragment were combined with conformers of the Tyr[1] residue and the Phe[3] side chain and minimized again. In this approach, the possible interactions of the Tyr[1] residue and the Phe[3] side chain with the cyclic backbone structure were not taken into account in the generation of low-energy conformers in the first stage. This approximation is supported by the fact that relative occupancies and chemical shifts of the two slowly exchangeable conformers observed for JOM-13 and its analogs in solution do not change significantly throughout a series encompassing numerous chemical modifications to the side chains of the first and third residues of JOM-13,[17] suggesting that these moieties do not influence the conformational properties of the 11-membered cycle in this tetrapeptide series.

In the first stage of the computations, all possible combinations of backbone torsion angles ϕ and ψ within the cycle CH_3CO-*cyclo*[D-Cys-Ala-D-Pen]OH (with a step of 30° within sterically allowed regions of the Ramachandran plot) and rotamers of D-Cys[2] and D-Pen[4] side chains ($\chi^1 = \pm 60°$ and 180°) were generated and minimized initially with the ECEPP/2 force field[23,24] using the program CONFORNMR.[25-27] "Soft" parabolic disulfide bond closing functions $U(r - r)^2$ were used with ECEPP/2 (U = 30 kcal/mol Å² for S–S bond and C^β–S–S valence angles) since it was observed that the use of the usual closing functions (U = 100 kcal/mol Å²) within the small, conformationally strained JOM-13 cycle led to an apparent increase of relative energy for some conformers which was inconsistent with results obtained with the CHARMm force field. Low-energy conformers identified in this fashion (ΔE < 10 kcal/mol) in which at least one torsion angle differed by >30° were selected and minimized additionally with the QUANTA 3.3/CHARMm force field.[28,29]

In the second stage of computations, the low-energy conformers of the fragment CH_3CO-*cyclo*[D-Cys-Ala-D-Pen]OH (ΔE < 4 kcal/mol with CHARMm) were combined with conformers of the Phe[3] side chain and Tyr[1] residue (including combinations of sterically allowed values for Tyr[1] ψ and D-Cys[2] ϕ torsion angles with a 50° step) and minimized again with the CHARMm force field. For all calculations, a compromise value of dielectric constant, ϵ = 10, was used and the adopted basis Newton-Raphson method of minimization was employed. This intermediate value of ϵ has previously been found to be appropriate for the conformational analysis of peptides[30,31] and for computations of electrostatic energy in proteins.[32] To assess the degree to which the computed low-energy conformers are dependent upon ϵ, JOM-13 conformer energies were recalculated using ϵ = 80, which resulted in only minor changes in relative energies, not exceeding 1.5 kcal/mol. The relative energies of the best representative conformations for structures A, B, and C are 0.2, 0.0, and 0.3 kcal/mol, respectively, with ϵ = 80, compared to 0.1, 0.0, and 1.3 kcal/mol with ϵ = 10 (see Table 1), in slightly worse agreement with NMR data.

Acknowledgment. This research was supported by the National Institute on Drug Abuse through Grants DA03910 (H.I.M.) and DA00118 (H.I.M.) and Contract DA30018 (NRL) and by the Office of Naval Research (NRL).

Supplementary Material Available: Tables of final positional parameters and U_{eq} values (equivalent isotropic thermal parameters) for all atoms, bond lengths and bond angles, and anisotropic thermal parameters (9 pages). This material is contained in many libraries on microfiche, immediately follows this article in the microfilm version of the journal, and can be ordered from the ACS; see any current masthead page for ordering information.

(23) Momany, F. A.; McGuire, R. F.; Burgess, A. W.; Scheraga, H. A. *J. Phys. Chem.* **1975**, *79*, 2361–2381.
(24) Nemethy, G.; Pottle, M. S.; Scheraga, H. A. *J. Phys. Chem.* **1983**, *87*, 1883–1887.
(25) Arseniev, A. S.; Lomize, A. L.; Barsukov, I. L.; Bystrov, V. F. *Biol. Membr. (USSR)* **1986**, *3*, 1077–1104.
(26) Lomize, A. L.; Sobol, A. G.; Arseniev, A. S. *Bioorg. Chem. (USSR)* **1990**, *16*, 179–201.
(27) Lomize, A. L.; Pervushin, K. V.; Arseniev, A. S. *J. Biomol. NMR* **1992**, *2*, 361–372.
(28) Brooks, B. R.; Bruccoleri, E. R.; Olafson, E. R.; States, D. J.; Swaminathan, S.; Karplus, M. *J. Comput. Chem.* **1983**, *4*, 187–217.
(29) Momany, F. A.; Rone, R. *J. Comput. Chem.* **1992**, *13*, 888–900.
(30) Lipkind, G. M.; Arkhipova, S. F.; Popov, E. M. *Int. J. Pept. Protein Res.* **1973**, *5*, 381–397.
(31) Popov, E. M. *Int. J. Quantum Chem.* **1979**, *XVI*, 707–737.
(32) Warshel, A.; Aqvist, J. *Annu. Rev. Biophys. Biophys. Chem.* **1991**, *20*, 276–298.